

RADIO IMAGING OF GAMMA-RAY BURST JETS IN NEARBY SUPERNOVAE

JONATHAN GRANOT AND ABRAHAM LOEB¹

Institute for Advanced Study, Einstein Drive, Princeton, NJ 08540; granot@ias.edu, loeb@ias.edu

Received 2003 May 21; accepted 2003 July 8; published 2003 July 28

ABSTRACT

We calculate the time evolution of the flux, apparent size, and image centroid motion of gamma-ray burst (GRB) radio jets and show that they can be resolved by the Very Long Baseline Array (VLBA) at distances of hundreds of megaparsecs. We find that GRB 030329, which showed spectroscopic evidence for an associated Type Ic supernova (SN) at a distance of ≈ 800 Mpc, might just be resolvable by VLBA after several months. The prospects are much better for jets that are oriented sideways in similar SNe with no GRB counterpart; in particular, the motion of the flux centroid in such jets can be detected by the VLBA up to $z \sim 1$, even when the jet cannot be resolved. If most GRBs are accompanied by a Type Ib/c SN, then there should be a few SN/GRB jets per year within a distance ≤ 200 Mpc, and most of them would be oriented sideways with no gamma-ray or X-ray precursor. Detection of these jets can be used to calibrate the fraction of all core-collapse SNe that produce relativistic outflows and determine the local GRB rate. Overall, the rate of Type Ib/c SNe that do not produce a GRB at all, but rather make relativistic radio jets with an initial Lorentz factor of a few, may be larger by up to 2 orders of magnitude than the rate of those that produce GRBs.

Subject headings: gamma rays: bursts — ISM: jets and outflows — supernovae: general

On-line material: color figures

1. INTRODUCTION

Recent evidence indicates that long-duration gamma-ray bursts (GRBs) are associated with Type Ic supernovae (SNe); of particular significance is the 3500–8500 Å spectrum of SN 2003dh associated with GRB 030329 (Stanek et al. 2003), which was very similar to that of SN 1998bw/GRB 020405 (Nakamura et al. 2001). This supports previous more circumstantial evidence, such as late time bumps in afterglow light curves (Bloom 2003) and the association of GRBs with central star-forming regions of galaxies (Bloom, Kulkarni, & Djorgovski 2002). This evidence raises two basic questions: (1) which fraction of all core-collapse SNe produces relativistic outflows, and (2) what is the probability distribution of the collimation angle, initial Lorentz factor, and energy output of these outflows?

For every nearby (≤ 1 Gpc) event like GRB 030329, there should be hundreds of GRB jets that are not pointed at us, based on existing estimates for the jet opening angle (Frail et al. 2001). As sufficiently close GRBs can be resolved by radio telescopes (Woods & Loeb 1999; Cen 1999; Granot, Piran, & Sari 1999; Ayal & Piran 2001; Paczyński 2001), an effective method to address the above two questions is to search for relativistic outflows in nearby core-collapse SNe. In § 2, we calculate the expected flux, apparent size, and image centroid motion of semirelativistic GRB radio jets viewed sideways. Such jets would have no observable GRB precursor but can be identified and timed via their associated SN emission. The early images of relativistic SN/GRB radio jets may resemble relativistic radio jets in quasars (Begelman, Blandford, & Rees 1984) or microquasars (Mirabel & Rodríguez 1999). However, while quasars often inject energy continuously into the jet, GRB sources are impulsive. Although quasar jets remain highly collimated throughout their lifetimes, GRB jets decelerate and expand significantly once they become nonrelativistic, ~ 1 yr after the explosion. The hydrodynamic remnant of a GRB even-

tually becomes nearly spherical after $\sim 5 \times 10^3$ yr (Ayal & Piran 2001).

2. FLUX, SIZE, AND CENTROID SHIFT OF GRB JETS

First, we calculate the radio flux from GRB jets observed from different viewing angles, θ_{obs} , with respect to the jet axis. We assume a double-sided jet and calculate the emission from both the forward jet that points toward the observer ($\theta_{\text{obs},1} \leq \pi/2$) and the opposite counterjet ($\theta_{\text{obs},2} = \pi - \theta_{\text{obs},1} \geq \pi/2$). Off-axis light curves from GRB jets were already calculated using different models with various degrees of complexity (Granot et al. 2002), varying from simple models (Dalal, Griest, & Pruet 2002; Rossi, Lazzati, & Rees 2002) to numerical simulations (Granot et al. 2001). Compared to simpler models, simulations typically show differences of order unity in the flux around or after the time of the peak in the light curve, a much more moderate rise in the flux before the peak, and a much smoother peak at $\theta_{\text{obs}} \leq 3\theta_0$, where θ_0 is the initial jet opening angle. The more moderate rise before the peak is due to relatively slow material at the sides of the jet, which emits much more isotropically compared to the front of the jet ($\theta \leq \theta_0$), where the emission is strongly beamed away from off-axis observers at early times. A simple model for the emission from the material behind the bow shock of GRB jets, which essentially addresses the same emission component, was also investigated by Wang & Loeb (2001).

For simplicity, we adopt an extended version of model 1 from Granot et al. (2002); where appropriate, we mention the qualitative differences that are expected in more realistic jet models. We assume a point source that moves along the jet axis. Its radial location R , the lab frame time t , and the observed time t_{obs} are related by $t_{\text{obs}} = t - R \cos \theta_{\text{obs}}$. For an on-axis observer ($\theta_{\text{obs}} = 0$), we assume a broken power-law spectrum (Sari, Piran, & Narayan 1998). The values of the peak flux and break frequencies before the jet break time t_j ($t_{\text{obs},j}$) are taken from Granot & Sari (2002).

At $t_j < t < t_{\text{NR}}$, where t_{NR} ($t_{\text{obs, NR}}$) is the nonrelativistic transition

¹ Guggenheim Fellow; on sabbatical leave from the Department of Astronomy, 60 Garden Street, Harvard University, Cambridge, MA 02138.

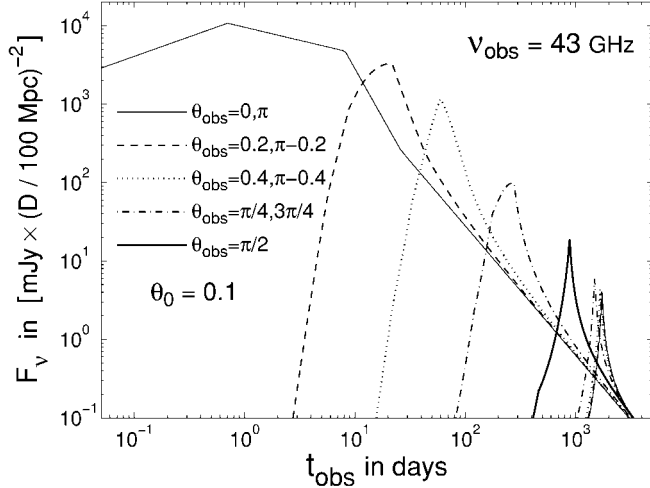


FIG. 1.—Radio light curves ($\nu_{\text{obs}} = 43$ GHz) for different viewing angles and $E = 10^{51}$ ergs, $n = 1 \text{ cm}^{-3}$, $\theta_0 = 0.1$, $\epsilon_e = 0.1$, $\epsilon_B = 0.01$, and $p = 2.5$. The jet that points toward us ($\theta_{\text{obs},1} \leq \pi/2$) and the counterjet that points away from us ($\theta_{\text{obs},2} = \pi - \theta_{\text{obs},1} \geq \pi/2$) are shown using the same line style (the emission from the counterjet peaks at a later time). The SN radio emission is expected to be much weaker in the plotted range of observed times. [See the electronic edition of the *Journal* for a color version of this figure.]

time, the temporal scaling of the peak flux and break frequencies is modified according to Rhoads (1999) and Sari, Piran, & Halpern (1999). At $t > t_{\text{NR}}$, the scalings are changed to those for the Sedov-Taylor regime (e.g., Frail, Waxman, & Kulkarni 2000). The light curve for off-axis observers is then calculated using the appropriate transformation of the radiation field, $F_\nu[\theta_{\text{obs}}, t_{\text{obs}}(\theta_{\text{obs}})] = a^3 F_{\nu/a}[0, t_{\text{obs}}(0)]$, where $a = (1 - \beta) / (1 - \beta \cos \theta_{\text{obs}})$. In Granot et al. (2002), it was also assumed that $t_{\text{obs}}(0)/t_{\text{obs}}(\theta_{\text{obs}}) = a$, which is an approximation, since actually $dt_{\text{obs}}(0)/dt_{\text{obs}}(\theta_{\text{obs}}) = a$ and is not very accurate for $t_j < t < t_{\text{NR}}$ when γ drops exponentially with radius. In this case, we must use the more accurate relation, $t_{\text{obs}} = t - R \cos \theta_{\text{obs}}$, where $R = \int_0^t \beta(\tilde{t}) d\tilde{t}$. The Lorentz factor is approximately given by $\gamma \approx \theta_0^{-1} (t/t_j)^{-3/2}$ at $t \leq t_j$, $\gamma \approx \theta_0^{-1} \exp(1 - t/t_j)$ at $t_j \leq t \leq t_{\text{NR}}$, and $\gamma \approx [1 - \beta_{\text{NR}}^2 (t/t_{\text{NR}})^{-6/5}]^{-1/2}$ at $t \geq t_{\text{NR}}$, where we use $\beta_{\text{NR}} = \beta(t_{\text{NR}}) \equiv 0.5$ ($\gamma_{\text{NR}} = 2/\sqrt{3} \approx 1.15$) for the transition to the nonrelativistic regime. We find

$$R \approx \begin{cases} [1 - (t/t_j)^3 \theta_0^2/16]ct, & t \leq t_j, \\ \{1 - [\exp(2t/t_j - 2) - 1/2](\theta_0^2 t_j/8t)\}ct, & t_j \leq t \leq t_{\text{NR}}, \\ R_{\text{NR}} + [(t/t_{\text{NR}})^{2/5} - 1](5/2)\beta_{\text{NR}} c t_{\text{NR}}, & t \geq t_{\text{NR}}, \end{cases} \quad (1)$$

where $R_{\text{NR}} = R(t_{\text{NR}})$. Following Sari et al. (1999), we use $t_{\text{obs}}(\theta_{\text{obs}} = 0) = R/4\gamma^2 c$ instead of $R/16\gamma^2 c$ and adopt their expression for $t_{\text{obs},j}(0)$ and the relation $t_j = 4t_{\text{obs},j}/\theta_0^2$. Using a simple energy equation, $E_{\text{iso}} = 2E/\theta_0^2 = (4\pi/3)nm_p c^2 R^3 \gamma^2$, and $t_{\text{NR}}/t_j = 1 - \ln x$, where $x \equiv \gamma_{\text{NR}} \theta_0$, we obtain²

$$R_j \equiv R(t_j) = \left(\frac{3E}{2\pi n m_p c^2} \right)^{1/3} = 6.8 \times 10^{17} \left(\frac{E_{51}}{n_0} \right)^{1/3} \text{ cm}, \quad (2)$$

² Here $f \approx 3$ for $\theta_0 = 0.1$ and has only a weak logarithmic dependence on θ_0 .

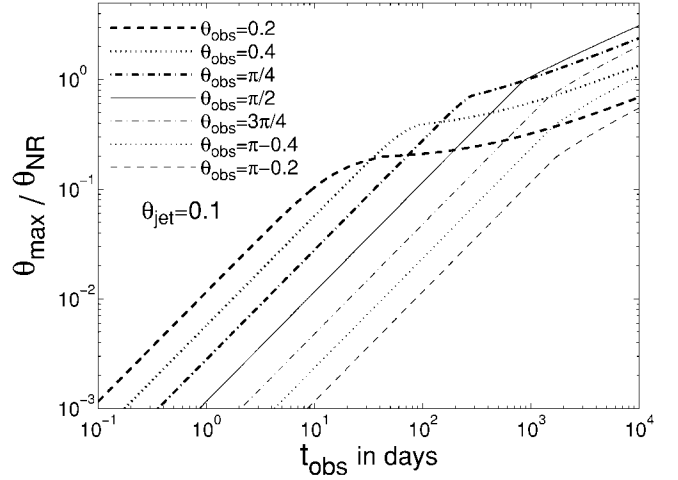


FIG. 2.—Angular extent of the jet, θ_{max} , in units of θ_{NR} (e.g., eq. [4]), for the same viewing angles and jet parameters as in Fig. 1. [See the electronic edition of the *Journal* for a color version of this figure.]

$$\frac{R_{\text{NR}}}{R_j} \equiv f = \frac{1 - \ln x - (x^{-2} - 1/2)\theta_0^2/8}{1 - \theta_0^2/16} \approx 1 - \ln x - \frac{1}{8\gamma_{\text{NR}}^2}, \quad (3)$$

where $n = n_0 \text{ cm}^{-3}$ is the external density and $E = 10^{51} E_{51}$ ergs is the energy in the two jets.

Figure 1 shows the radio light curves at different θ_{obs} , for both the forward jets and the counterjets. While the optical is typically above the peak frequency ν_m at t_j , the radio is typically below ν_m , and therefore the temporal decay slope $\alpha = -d \ln F_\nu / d \ln t_{\text{obs}}$ for $\theta_{\text{obs}} < \theta_0$ changes from $-1/2$ to $1/3$ at $t_{\text{obs},j}$. After $t_{\text{obs},m}$ when ν_m sweeps past the observed frequency ν_{obs} , $\alpha = p$, while at $t > t_{\text{NR}}$ $\alpha = (15p - 21)/10$, where $p \sim 2-2.5$ is the power-law index of the electron energy distribution. For $\theta_{\text{obs}} > \theta_0$, the flux still rises at $t_{\text{obs},j} < t_{\text{obs}} < t_{\text{obs},m}$; for $\theta_{\text{obs}} \lesssim \pi/4$, the flux peaks at $t_{\text{obs},p} = t_{\text{obs},m}$, while for $\theta_{\text{obs}} \geq \pi/4$, $t_p = t_{\text{NR}}$. If $t_{\text{obs},p} = t_{\text{obs},m}$, the spectral slope should change from $F_\nu \propto \nu^{1/3}$ to $\nu^{(1-p)/2}$ at $t_{\text{obs},p}$, which should be easy to observe. If $t_p = t_{\text{NR}}$, then $t_{\text{obs},p} \sim t_{\text{obs},j} (\theta_{\text{obs}}/\theta_0)^2 \sim t_{\text{NR}} \theta_{\text{obs}}^2/4$ for $\theta_0 < \theta_{\text{obs}} \ll 1$, while for the counterjet $t_{\text{obs},p} \sim t_{\text{NR}}$, so that the ratio of the two peak times is $\sim 4/\theta_{\text{obs}}^2$ and may be used to estimate θ_{obs} . For $\theta_{\text{obs}} \geq \pi/4$, $t_{\text{obs},p}$ for the two jets is less than a factor of ~ 10 apart. The light curves for the counterjets with $\theta_{\text{obs},2} \geq 3\pi/4$ ($\theta_{\text{obs},1} \leq \pi/4$) are all very similar and peak at $\sim 2R_{\text{NR}}/c \approx 2t_{\text{NR}}$.

For $\theta_{\text{obs}} > \theta_0$, the peak flux is a factor of a few larger than the flux for $\theta_{\text{obs}} = 0$ at the same t_{obs} . For more realistic jet models, we expect a much smoother peak and a somewhat smaller peak flux. We note that $F_\nu(t_{\text{NR}}) \propto E$ (Frail et al. 2000), so that a larger energy implies a larger flux at t_{NR} . For example, keeping the same energy per solid angle and increasing θ_0 from 0.1 to 0.3 (0.5) would increase E and therefore $F_\nu(t_{\text{NR}})$ by a factor of 9 (25) and would modify the afterglow light curves (Granot et al. 2002).

Figure 2 shows the maximal angular size³ θ_{max} of the jets and counterjets from Figure 1 in units of

$$\theta_{\text{NR}} = \frac{R_{\text{NR}}}{D} = 1.4 \frac{f}{3} \left(\frac{E_{51}}{n_0} \right)^{1/3} \left(\frac{D}{100 \text{ Mpc}} \right)^{-1} \text{ mas}, \quad (4)$$

³ If both the forward jets and the counterjets are visible, the total angular size would be the sum of their two θ_{max} .

measured from the center. The Very Long Baseline Array (VLBA) has an angular resolution of⁴ $\sim 170 \mu\text{as}$ at 43 GHz and may resolve the jet around t_{NR} (typically a few months to years after the SN), up to distances of $D \sim 1$ Gpc. The expected peak flux at 43 GHz for a jet with $\theta_{\text{obs}} \sim \pi/4$ at $D \sim 1$ Gpc is ~ 1 mJy.

The apparent velocity of the source on the sky is $v_{\text{ap}} \equiv (d\theta_{\text{max}}/dt_{\text{obs}})D \approx R \sin \theta_{\text{obs}} / (t - R \cos \theta_{\text{obs}})$. For $t \ll t_j$, $v_{\text{ap}} \approx \text{const}$ (see inset of Fig. 3) and is $\approx c$ for $\theta_{\text{obs}} = \pi/2$, subluminal for $\theta_{\text{obs}} > \pi/2$, and superluminal for $\theta_{\text{obs}} < \pi/2$. For $\theta_{\text{obs}} \ll 1$, we obtain $v_{\text{ap}} \sim 2c\theta_{\text{obs}} / (\theta_{\text{obs}}^2 + 1/8\gamma^2)$, which for $\theta_{\text{obs}} > 1/\gamma$ is $\sim 2c/\theta_{\text{obs}}$. For $\theta_{\text{obs}} \leq 1/\gamma$, we do not obtain the familiar result $v_{\text{ap}} \sim \gamma c$ for the afterglow image, since we consider a point source at a fixed angle θ from our line of sight, while the edge of an afterglow image viewed on-axis is at $\theta \sim 1/\gamma$, where γ changes with time (substituting $\theta_{\text{obs}} \sim 1/\gamma$ in our formula reproduces this result). However, we are interested mainly in $\theta_{\text{obs}} > \theta_0$, for which our simple estimate of the source size is reasonable. When γ becomes $\leq 1/\theta_{\text{obs}}$, v_{ap} begins to decrease. At this stage, if the jet expands sideways significantly (i.e., $\theta_{\text{jet}} \sim 1/\gamma$) and if the emission from the whole jet is taken into account, then $v_{\text{ap}} \sim \gamma c$ and $\theta_{\text{max}}(t_{\text{NR}}) \sim \theta_{\text{NR}}$ for all θ_{obs} and not just for $\theta_{\text{obs}} \geq \pi/4$. Just how $\theta_{\text{max}}(t_{\text{NR}})$ changes with θ_{obs} depends on how close to spherical the jet is at t_{NR} . Numerical simulations show that the jet does not expand laterally very much before t_{NR} and may approach spherical symmetry only long after t_{NR} (Granot et al. 2001; Ayal & Piran 2001).

Figure 3 shows the angular location of the flux centroid (FC) θ_{cent} . Our results are consistent with those of Sari (1999) for $\theta_{\text{obs}} < \theta_0$ and $t < t_{\text{NR}}$. The inset shows $d\theta_{\text{cent}}/dt_{\text{obs}} = v_{\text{ap}}/D$ for $D = 100$ Mpc. Because of symmetry, $\theta_{\text{cent}} \equiv 0$ for $\theta_{\text{obs}} = 0, \pi/2$. At $t < t_{\text{NR}}$, the forward jet is much brighter than the counterjet for $\theta_{\text{obs}} \leq \pi/4$, and the FC largely follows the forward jet. However, when the counterjet peaks at $\sim t_{\text{NR}}$, it becomes somewhat brighter than the forward jet, so that the FC gets closer to the location of the counterjet (as may be seen from the negative values of θ_{cent} in Fig. 3). After t_{NR} , the forward jets and counterjets have almost the same brightness and the FC moves very close to the location of the SN, which is midway between the two jets. This implies a rather large change in the location of the FC $\sim \theta_{\text{NR}}$ for $\theta_{\text{obs}} \sim \pi/4$, near t_{NR} . For a more realistic jet model, the peak of the counterjet light curve is expected to be flatter and at a somewhat lower flux level, so that it is less clear if it will peak above the emission from the forward jet. Therefore it is not obvious whether θ_{cent} will actually obtain negative values near t_{NR} . However, the main conclusion, that a large change in θ_{cent} of $\sim \theta_{\text{NR}}$ for $\theta_{\text{obs}} \sim \pi/4$ is expected near t_{NR} over a timescale $\Delta t_{\text{obs}} \leq t_{\text{obs}}$, as well as the conclusion that θ_{cent} approaches zero at $t > t_{\text{NR}}$, is robust (unless the two jets are not identical or encounter a different external density).

The best rms error on the localization of the FC was reported as $10 \mu\text{as}$ (Fomalont & Kopeikin 2003). Such an accurate localization requires a nearby bright radio quasar on the sky. Compared to the best available angular resolution, θ_{cent} can be determined with an accuracy better by a factor of ~ 10 – 20 . Therefore, the movement of the FC on the sky may be detected even when the jet is not resolved (i.e., at early times, $t \ll t_{\text{NR}}$ for relatively nearby sources, or near t_{NR} for more distant sources potentially up to cosmological distances, $z \sim 1$, although such sources would be dim at that age, ~ 0.1 mJy).

At sufficiently late times, $\geq t_{\text{NR}} \sim 1$ yr, when the jets become nonrelativistic and begin to approach a spherical configuration, one may estimate their physical parameters, i.e., E , n , and the

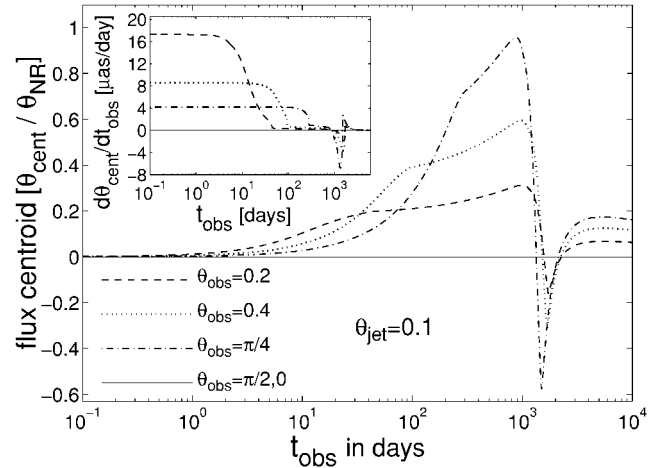


FIG. 3.—Angle of the FC relative to the center of the SN explosion, θ_{cent} , along the projection of the forward jet (with $\theta_{\text{obs}} < \pi/2$) on the sky, in units of θ_{NR} (e.g., eq. [4]). The inset shows $d\theta_{\text{cent}}/dt_{\text{obs}}$ for $D = 100$ Mpc. [See the electronic edition of the Journal for a color version of this figure.]

equipartition parameters for the electrons (ϵ_e) and the magnetic field (ϵ_B), in a similar way as was done for GRB 970508 by Frail et al. (2000). This can help constrain the structure of GRB jets and test if they are uniform or vary smoothly.

3. APPLICATION FOR GRB 030329

GRB 030329 was detected at a very low redshift of $z = 0.1685$ (Greiner et al. 2003) or an angular distance $D \approx 590$ Mpc. Despite its low energy output in gamma rays, bumps in its optical afterglow light curve provide evidence for later energy injection by refreshed shocks that bring the energy of the afterglow shock close to its average value for all GRBs (Granot, Nakar, & Piran 2003). Thus, we expect $E_{51} \approx 1$. Since the prompt GRB was observed, $\theta_{\text{obs}} \leq \theta_0$ and the emission from the counterjet should peak at $\sim 2t_{\text{NR}} \approx 2R_{\text{NR}}/c \sim 5(E_{51}/n_0)^{1/3}$ yr, at a flux of $\sim 20 \mu\text{Jy}$, which would be difficult to detect. However, $t_{\text{obs, NR}}$ for the forward jet could be somewhat earlier, around a few months, because of light-travel effects and since the jet is still mildly relativistic at t_{NR} . If the jet spreads sideways significantly during the relativistic phase ($\theta_{\text{jet}} \sim 1/\gamma$), then its angular size after a few months should be $\sim \theta_{\text{NR}} \sim 270(E_{51}/n_0)^{1/3} \mu\text{as}$, which just might be resolved by the VLBA. However, if the lateral spreading of the jet during the relativistic stage is modest, the jet might be resolvable only after a few years when it becomes more spherical but rather dim (a few tens of microjanskys). The expected shift in the FC from early times to several months may be up to an angle of $\sim \sin \theta_{\text{obs}} \theta_{\text{NR}} \leq \theta_0 \theta_{\text{NR}} \approx 19(E_{51}/n_0)^{1/3} \mu\text{as}$, which might just be detectable with the VLBA if $\theta_{\text{obs}} \approx \theta_0$.

4. COMPARING THE RATE OF SUPERNOVAE Ib/c AND GRBs

The rate of Type Ib/c SNe (SNe Ib/c) in spiral galaxies is estimated to be ~ 0.2 per century per $10^{10} L_{B, \odot}$ (Prantzos & Boissier 2003). The luminosity density of the local universe (Glazebrook et al. 2002; Blanton et al. 2003), $\sim 10^8 L_{B, \odot} \text{Mpc}^{-3}$, implies a rate density of SN Ib/c of $\sim 2 \times 10^4 \text{Gpc}^{-3} \text{yr}^{-1}$. The collimation-corrected rate of GRBs is estimated to be (Frail et al. 2001) $\sim 250 \text{Gpc}^{-3} \text{yr}^{-1}$. Hence, only $\sim 1\%$ of all SNe Ib/c may be associated with GRBs.⁵

⁵ Norris 2002 has a more optimistic prediction that $\geq 25\%$ of all SNe Ib/c produce a subclass of low-luminosity GRBs similar to GRB 980425/SN 1998bw.

⁴ See <http://www.aoc.nrao.edu/vlba/obstatus/obssum/node30.html>.

However, more SNe may have relativistic outflows with low Lorentz factors that would not result in GRBs (which require an initial Lorentz factor $\Gamma_0 \geq 100$) but rather in UV (for $\Gamma_0 \sim 10$) or radio (for $\Gamma_0 \leq 3$) transients only. The observational constraints on the rates of such transients are weak. Calibration of the statistics of relativistic radio jets in core-collapse SNe can be used to infer the rate of such transients (which should occur on the rare occasions when the same jets are viewed on-axis). It can also provide new and more reliable evidence for the collimation of GRB jets and an independent estimate for the distribution of the collimation angles.

5. CONCLUSIONS

We have calculated the radio light curves and the evolution of the apparent size and FC of GRB jets viewed sideways. As the jets do not point at us, they will have no gamma-ray precursor but will instead be preceded by an SN Ib/c. An ~ 1 yr old GRB remnant at $D \sim 100$ Mpc is predicted to have a characteristic radio flux of ~ 100 mJy, an image size of ~ 1 mas, and FC motion of $\sim 20 \mu\text{s week}^{-1}$. Such a source can be resolved by the VLBA at $D \leq 1$ Gpc, while the motion of its FC might be monitored up to $z \sim 1$ (although at $z \sim 1$ it would be very dim, ~ 0.1 mJy). The apparent size of the jet or superluminal motion of its FC within the first few months after the SN may provide evidence for relativistic motion.

A relativistic jet of length ct may also serve as a yardstick for constraining cosmological parameters. However, the required precision for this purpose may not be attainable if the jet orientation is not well known or the surrounding medium is inhomogeneous.

For an off-axis jet, there should be a time-dependent linear polarization, which peaks near the time of the peak in the light curve and slowly decreases with time as the jet becomes more spherical and symmetric around the line of sight (Granot et al. 2002). If the jet is resolved, then polarization maps could be generated, as is commonly done for extragalactic radio jets. This could reveal the magnetic field geometry and orientation in the jet and whether it has a large-scale ordered component (Granot & Königl 2003).

The existence of an early phase during which the emission of the jet peaked in the UV ($\gamma \geq 10$) can in principle be inferred

from the ionization cones preceding the jet in the surrounding gas (Perna & Loeb 1998). Since the recombination time of the gas is $\sim 10^5 n_0^{-1}$ yr, these cones should exist for long times after the SN explosion. However, the separation between the ionization fronts and the edges of the jet grows large only after the jet becomes nonrelativistic. At these late times, one may detect emission lines from highly ionized metal-rich gas (Perna, Raymond, & Loeb 2000) that reflect the hardness of the emission spectrum of the jet at earlier times, when it was highly relativistic. Detection of ionization cones can be used to infer the early opening angle and spectral flux of the jet at different frequencies (corresponding to the ionization state of different ions). The latter can be used to estimate the initial Lorentz factor of the jet, Γ_0 , in the range ~ 5 – 20 , or determine if $\Gamma_0 \leq 5$ (no ionization cones) or $\Gamma_0 \geq 20$ (ionizing extending up to soft X-rays).

There is strong evidence connecting GRBs with Type Ic SNe that have a large kinetic energy, $\geq 10^{52}$ ergs (termed “hypernovae” by Paczyński 1998), and have a distinct spectral signature, as was observed for SN 1998bw and SN 2003dh. The search for GRB radio jets in SNe with such a spectrum is particularly interesting, as it could show whether all such SNe produce GRBs. For $\theta_{\text{obs}} < \theta_0$, the existence of relativistic jets can be revealed by their high brightness temperatures ($\gg 10^{11}$ K, e.g., Kulkarni et al. 1998; Li & Chevalier 1999). The fraction of SNe Ib/c that produce GRB jets can help determine the local GRB rate and the distribution of θ_0 .

It may prove interesting to search for a correlation between the value of Γ_0 as estimated from the ionization cones and the spectrum of the SN. A correlation with ejecta energy and abundance patterns (Maeda & Nomoto 2003) may show a continuous change in the SN spectrum as a function of Γ_0 of the bipolar jets, which might indicate that these jets are intimately related to, or perhaps are, the main cause of the SN explosion.

We thank Josh Winn, Mark Reid, and Re'em Sari for useful discussions. This work was supported in part by the Institute for Advanced Study (IAS), funds for natural sciences (J. G.), and NSF grants AST 00-71019 and AST 02-04514 and NASA grant NAG5-13292 (A. L.). A. L. acknowledges support from the IAS at Princeton and the J. S. Guggenheim Memorial Fellowship.

REFERENCES

- Ayal, S., & Piran, T. 2001, *ApJ*, 555, 23
 Begelman, M. C., Blandford, R. D., & Rees, M. J. 1984, *Rev. Mod. Phys.*, 56, 255
 Blanton, M. R., et al. 2003, *ApJ*, 592, 819
 Bloom, J. 2003, in *Proc. Gamma Ray Bursts in the Afterglow Era*, in press (astro-ph/0303478)
 Bloom, J. S., Kulkarni, S. R., & Djorgovski, S. G. 2002, *AJ*, 123, 1111
 Cen, R. 1999, *ApJ*, 524, L51
 Dalal, N., Griest, K., & Pruet, J. 2002, *ApJ*, 564, 209
 Fomalont, E. B., & Kopeikin, S. M. 2003, preprint (astro-ph/0302294)
 Frail, D. A., et al. 2001, *ApJ*, 562, L55
 Frail, D. A., Waxman, E., & Kulkarni, S. R. 2000, *ApJ*, 537, 191
 Glazebrook, K., et al. 2003, *ApJ*, 587, 55
 Granot, J., & Königl, A. 2003, *ApJ*, submitted (astro-ph/0304286)
 Granot, J., Nakar, E., & Piran, T. 2003, preprint (astro-ph/0304563)
 Granot, J., Panaitescu, A., Kumar, P., & Woosley, S. E. 2002, *ApJ*, 570, L61
 Granot, J., Piran, T., & Sari, R. 1999, *ApJ*, 513, 679
 Granot, J., & Sari, R. 2002, *ApJ*, 568, 820
 Granot, J., Miller, M., Piran, T., Suen, W. M., & Hughes, P. A. 2001, in *Gamma-Ray Bursts in the Afterglow Era*, ed. E. Costa, F. Frontera, & J. Hjorth (Berlin: Springer), 312
 Greiner, J., et al. 2003, *GCN Circ.* 2020 (<http://gcn.gsfc.nasa.gov/gcn/gcn3/2020.gcn3>)
 Kulkarni, S. R., et al. 1998, *Nature*, 395, 663
 Li, Z.-Y., & Chevalier, R. A. 1999, *ApJ*, 526, 716
 Maeda, K., & Nomoto, K. 2003, *ApJ*, submitted (astro-ph/0304172)
 Mirabel, I. F., & Rodríguez, L. F. 1999, *ARA&A*, 37, 409
 Nakamura, T., Mazzali, P. A., Nomoto, K., & Iwamoto, K. 2001, *ApJ*, 550, 991
 Norris, J. P. 2002, *ApJ*, 579, 386
 Paczyński, B. 1998, *ApJ*, 494, L45
 ———. 2001, *Acta Astron.*, 51, 1
 Perna, R., & Loeb, A. 1998, *ApJ*, 501, 467
 Perna, R., Raymond, J., & Loeb, A. 2000, *ApJ*, 533, 658
 Prantzos, N., & Boissier, S. 2003, *A&A*, 406, 259
 Rhoads, J. E. 1999, *ApJ*, 525, 737
 Rossi, E., Lazzati, D., & Rees, M. J. 2002, *MNRAS*, 332, 945
 Sari, R. 1999, *ApJ*, 524, L43
 Sari, R., Piran, T., & Halpern, J. P. 1999, *ApJ*, 519, L17
 Sari, R., Piran, T., & Narayan, R. 1998, *ApJ*, 497, L17
 Stanek, K. Z., et al. 2003, *ApJ*, 591, L17
 Wang, X., & Loeb, A. 2001, *ApJ*, 552, 49
 Woods, E., & Loeb, A. 1999, preprint (astro-ph/9907110)